GEOLOGICA CARPATHICA, 54, 5, BRATISLAVA, OCTOBER 2003
317–328

MINERAL AND CHEMICAL COMPOSITION OF MANGANESE HARDGROUNDS IN JURASSIC LIMESTONES OF THE WESTERN CARPATHIANS

IGOR ROJKOVIČ[1], ROMAN AUBRECHT[2] and MILAN MIŠÍK[2]

[1] Department of Mineral Deposits, Faculty of Natural Sciences, Comenius University, Mlynská dolina, 842 15 Bratislava, Slovak Republic; rojkovic@nic.fns.uniba.sk
[2] Department of Geology and Paleontology, Faculty of Natural Sciences, Comenius University, Mlynská dolina, 842 15 Bratislava, Slovak Republic; aubrecht@nic.fns.uniba.sk

(Manuscript received June 6, 2002; accepted in revised form March 11, 2003)

Abstract: Manganese crusts and nodules in Jurassic limestones correspond to those formed on recent submarine pelagic or hemipelagic non-deposition surfaces and hardgrounds. The ore mineralization is represented by pyrolusite, romanèchite, manganite, and iron hydroxides. The structure of the manganese minerals, Mn/Fe and Si/Al ratio and Co, Cu, Ni and REE distribution in the ores indicate hydrogenetic and diagenetic accumulation of manganese minerals. Later, Cretaceous supergene accumulation filled fissures and cavities in the limestones.

Key words: Tethys, Jurassic, manganese minerals, hardgrounds, chemical composition.

Introduction

Jurassic sections in the Alpine-Mediterranean region show transitions from Bahama-type carbonates through red nodular limestones (Rosso Ammonitico), to deep oceanic pelagic limestones and radiolarites. Manganese nodules and crusts formed near the continental margin on seamounts during high sea-level are characteristic for the Jurassic period in the Northern Calcareous Alps, Sicily, Betic Cordillera and other parts of the Tethys region (Jenkyns 1970; German 1972; Drittenbass 1979; Jenkyns et al. 1991; Roy 1980; Vera & Martín-Algarra 1994; Jimenez Espinosa et al. 1997; DiStefano & Mindszenty 2000).

Manganese in pelagic carbonates indicates major tectonic events during geodynamic evolution of the Jurassic continental margin of the Tethys-Ligurian Sea. The main transgressive phases (Early Toarcian, Late Aalenian to Bajocian and Late Bathonian to Callovian) are marked by a manganese content increase whereas the regressive phases (Late Pliensbachian, Late Toarcian to Middle Aalenian, Early Bathonian to Middle Bathonian, Oxfordian) are characterized by decreasing trends (Corbin et al. 2000). Such occurrences are common in the Jurassic limestones of the Western Carpathians (Rakús 1987).

Black manganese crusts ("hardgrounds") of small extent and mostly several centimetres thick are known in the Klippen Belt near Vršatec, Babiná, Bolešov, Kyjov-Pusté Pole and Drieňová hora Hill (Mišík 1979, 1994; Mišík & Sýkora 1993). The crust from Babiná contains Mn-Fe oxides with 17 % of MnO and 15 % of Fe_2O_3 (Mišík et al. 1994). In the Bolešovská dolina Valley, between Nemšová and Pruské, Aubrecht et al. (1998) have described Fe-Mn crust ("hardground" and nodules) 1–5 cm thick in the Upper Callovian-Lower Oxfordian limestone near Bolešov in the Czorsztyn Unit. They identified here ranciéite, goethite and hematite with the help of X-ray diffraction.

Other important occurrences of manganese ores were exploited during the First World War near Mikušovce. Manganese ore with ammonites occurs in deep pelagic to shallow neritic sea sediments (Andrusov et al. 1955). Two types of manganese ores were identified in the area of Mikušovce (Andrusov et al. 1955) and later in Lednica castle within the Pieniny Klippen Belt (Mišík & Rojkovič 2002). The first one is low-grade ore and belongs to syngenetic accumulations of the hardground type in red nodular Callovian-Oxfordian limestones. The second one represents high-grade ore filling clefts in the crinoidal Bathonian limestones at the locality Mikušovce and small caverns in the Kimmeridgian-Lower Tithonian limestone at the locality Lednica (Mišík & Rojkovič 2002). Pyrolusite, psilomelane and wad were found in the ore (Andrusov et al. 1955). Čechovič (1942) proposed sedimentary origin of the deposit with later metasomatic alteration of limestone. However, cherts as well as manganese ores were of sedimentary-diagenetic origin according to Andrusov et al. (1955). Formation of the ore was contemporaneous with the accumulation of ammonites in the "Upper Dogger and Lower Malm" and filling of fissures in the Bajocian was either of hydrometasomatic or infiltration origin (Andrusov et al. 1955). The aim of this paper is to include new data and ideas on manganese mineralization in the limestones of this region since the last paper was published in 1955.

Geological setting

Jurassic manganese hardgrounds in the Western Carpathians are related to periods of transgressions and sea-level highstands. Such were the periods of Late Sinemurian, Toarcian and Callovian–Oxfordian. The Liassic hardgrounds are mostly ferroan; the manganese hardgrounds were only found in the Nedzov Nappe of the Čachtické Karpaty Mts (Chtelnica

— Late Sinemurian, Hrušové, Bzince pod Javorinou — Toarcian). The Callovian-Oxfordian manganese hardgrounds are common in the Czorsztyn Unit of the Pieniny Klippen Belt (localities Bolešov, Horné Sŕnie, Mikušovce and Vršatec, Fig. 1). For comparison, a few samples of Albian age (Kamenica and Jarabiná, both Czorsztyn Unit) were studied. The Albian hardgrounds in the Czorsztyn Unit were formed in similar eustatic regime as the Middle Jurassic ones. Their development was also characterized by rapid sea-level rise, with condensed sedimentation and formation of phosphatic, manganese and ferroan stromatolitic crusts.

The Nedzov Nappe belongs to the Hronic Unit, but has common features with originally more southern units of the Silicicum (Mello in Salaj et al. 1987). The Jurassic-Lower Cretaceous sequence, named as Hrušové Group, represents sediments deposited in a relatively shallow-water environment. The Liassic is represented by cherty crinoidal limestones. Later, the Fe-Mn condensed crust was formed in the Toarcian (Fig. 2). It is overlain by pseudonodular limestones with cherts (Middle-Upper Jurassic). The Upper Jurassic is represented by micritic limestones with layers of allodapic limestones (Barmstein Limestones — Mišík & Sýkora 1982).

The Pieniny Klippen Belt (PKB) is the most complicated tectonic unit of the Western Carpathians. It is a narrow belt extending from the Vienna Basin for over 600 km, through southern Poland, eastern Slovakia and Transcarpathian Ukraine as far as northern Romania. This zone is less than 15 km wide. It is tectonically separated from the Flysch Belt to the north and from the Central Western Carpathians to the south. It is composed of Jurassic, Cretaceous and Paleogene sequences. This zone was affected by at least two major deformation phases. The first phase, which formed Laramian nappe structure occurred in the latest Cretaceous and earliest Paleogene. The second one, which disturbed the previous structure, was an Oligocene-Early Miocene orogenic phase, dominated by lateral movement and transpressional deformation in a large shear-zone. This process created the recent, unique klippen structure, where limestone successions (mostly Jurassic to Early Cretaceous) form blocks and tectonic slices enveloped by softer marlstones and claystones (predominantly Late Cretaceous). The crystalline basement of these sedimentary units is not known; it was most probably consumed by underthrusting beneath the Central Carpathian block. Despite this extensive tectonic deformation, the Pieniny Klippen Belt has almost no metamorphic or thermal overprint and its sequences have perfectly preserved fossils and sedimentary structures.

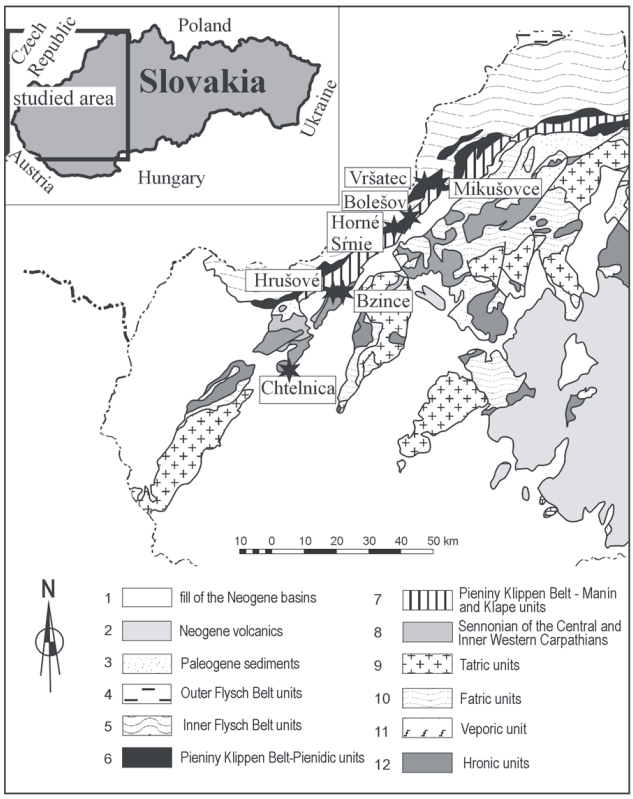

Fig. 1. Location of the studied manganese hardgrounds in the Western Carpathians.

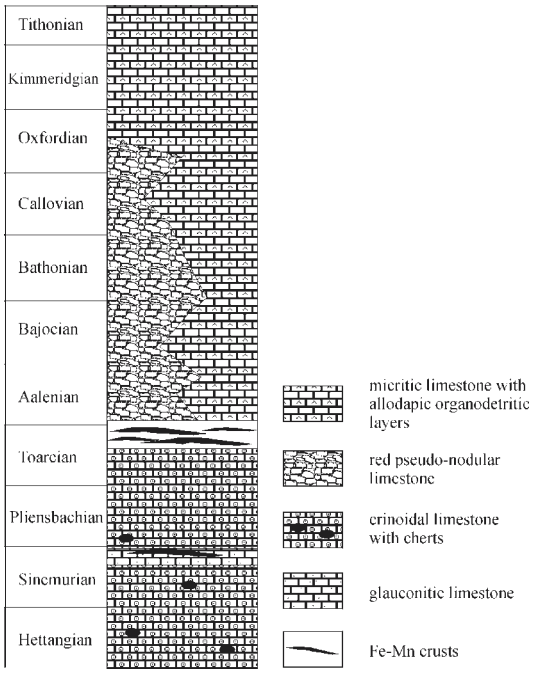

Fig. 2. Jurassic lithostratigraphy of the Nedzov Nappe.

All the PKB localities studied herein belong to the Czorsztyn Unit, which formed a pelagic swell during the Jurassic period (a hypothetical Czorsztyn Swell sensu Mišík 1994; = Ridge — sensu Birkenmajer 1986, 1988). In the Aalenian, the sedimentary area lacked vertical contrast and deposition of marlstones and claystones was dominant at that time (Harcygrund Shale and Skrzypny Shale Formations according to Birkenmajer 1977). Uplift of the Czorsztyn Swell was strongly accentuated in the Bajocian and resulted in deposition of a white crinoidal limestone (Smolegowa Limestone Formation) followed by red crinoidal limestone (Krupianka Limestone Formation). After a gradual sea-level rise during the latest Bajocian and Bathonian to Oxfordian, the deposition of the crinoidal limestone gave way to pelagic red nodular Ammonitico Rosso-type limestones of the Czorsztyn Limestone Formation, which was widespread in the Czorsztyn Unit between the Callovian and Late Tithonian. Some non-nodular equivalents of the Czorsztyn Limestone Formation are locally observed

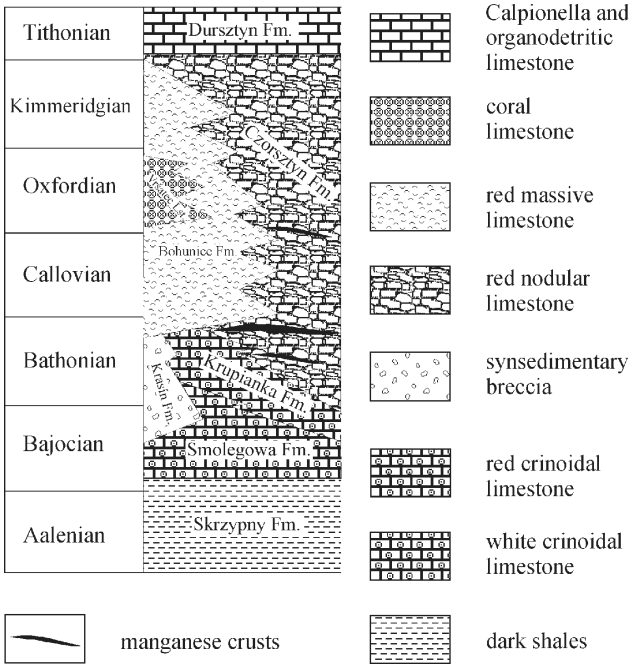

Fig. 3. Lithostratigraphic scheme of the Czorsztyn Unit.

(Andrusov 1945, p. 17). This relatively uncondensed variety was later named the Bohunice Limestone Formation by Mišík et al. (1994). The time of the sedimentation regime change from crinoidal limestones to Czorsztyn or Bohunice Limestones was associated with condensed sedimentation, mainly at the base of the latter formations. At this time, pronounced formation of manganese crusts took place (Fig. 3).

Studied localities

Chtelnica

The locality occurs 2.5 km north of the village of Chtelnica, on the NW slope of Holý vrch Hill. The locality was found by Peržel (1966). Poor outcrops do not allow a complete reconstruction of the Liassic sequence. There are probably three units: 1. Grey to greenish, fine-grained crinoidal limestone with glauconite and numerous ammonites (Sinemurian), 2. pink, brownish to grey organodetrital micritic limestones (Upper Lotaringian), 3. pink micritic limestone (probably Toarcian). Most likely, Fe-Mn crust debris and nodules found in the lower part of the slope belong to the latter unit (Fig. 4.1). In the crust, some recrystallization features, bivalve borings (Fig. 4.2) and brecciation were observed.

Hrušové

The locality is an abandoned quarry in the Rubanina Valley in the Čachtické Karpaty Mts, 500 m SSE from the village Hrušové. A hardground consisting of a crust about 5 cm thick has been known for a long time. The beds are tectonically overturned. Jurassic of the Choč Nappe is uncovered in the quarry. Hanáček (in Salaj et al. 1987) attributed this succession to Hrušové Group of the Nedzov Nappe. More recently, the locality was described by Kullmanová & Gašpariková (1983, p. 56), where a stratigraphic position of these deposits is mentioned. The stratigraphic base is represented by white and pink crinoidal biosparites (Liassic, maximum Lower Toarcian). The hardground occurs at the boundary between the crinoidal limestones (at the contact with Mn-hardground, the crinoidal ossicles have scalenohedral edges) and red nodular to pseudonodular limestones (equivalent of Klaus or Reitmauer Limestone Formation). The original, lower part of the hardground crust is black (manganese), whereas the original upper part is brown (ferroan, Fig. 4.3). Their boundary is undulated, reminding plastic deformation. The brown part is structureless or it forms a stromatolitic structure up to 4 cm thick. It contains abundant encrusting foraminifers. The hardground crust yielded the following Late Toarcian to Middle Bajocian fossils (Kullmanová & Gašpariková 1983): *Phylloceras* cf. *kunthi*, *Ptychophylloceras* sp., *Caliphylloceras* sp., *C.* cf. *connectens*, *Lytoceras* sp., *Pseudogrammoceras fallaciosum, ?Leioceras* sp., *Tmetoceras scissum, Chondroceras* sp. and Toarcian gastropod *Pleurotomaria mulsanti* (Thiolliere). The overlying red nodular limestone yielded an ammonite *Leptoceras* (*Vermisphinctes*) which ranges from Bajocian to Early Bathonian.

Bzince pod Javorinou

A quarry near the village of Bzince pod Javorinou was illustrated by Hanáček (in Salaj et al. l987). Directly overlying Liassic crinoidal limestones, a limonitized limestone layer occurs, with Fe-Mn oncoids. Algal and bivalvian borings are present in the hardground. The hardground forms a basis for the pseudonodular Adnet Limestone (Kullmanová & Gašpariková 1983). The probable age of the hardground is Late Toarcian.

Bolešov

A klippe of the Czorsztyn Unit occurs at the end of the Bolešovská dolina Valley west of Bolešov village in the Middle Váh Valley. It was for the first time described by Salaj (1987, 1990, 1997) and later by Aubrecht et al. (1998). Over a thick bedded to massive, white to yellowish sandy crinoidal limestone (Smolegowa Limestone, Bajocian–Lower Callovian) a dark violet to black-reddish limestone occurs with a 1–5 cm thick brown to black crust (Fe-Mn hardground). The hardground contains Fe-Mn stromatolites, rarely domatic with radial partition and oncoids (Upper Callovian–Lower Oxfordian). Higher up, it is followed by pink-violetish limestone with black-coated (Mn oxides) bivalve shells (Bohunice Limestone). This limestone is overlain by creamy micritic limestone (Sobótka Limestone) with red-coated tiny intraclasts (Upper Tithonian).

Horné Sŕnie

A manganese crust with stromatolites was found in Bohunice Limestone within the easternmost of the quarries of Horné Sŕnie cement factory, at Ostrá hora Hill. The limestone contains numerous foraminifers *Globuligerina* sp. and calcareous dinocysts *Colomisphaera fibrata* Nagy indicating an Oxfordian age for the manganese crust.

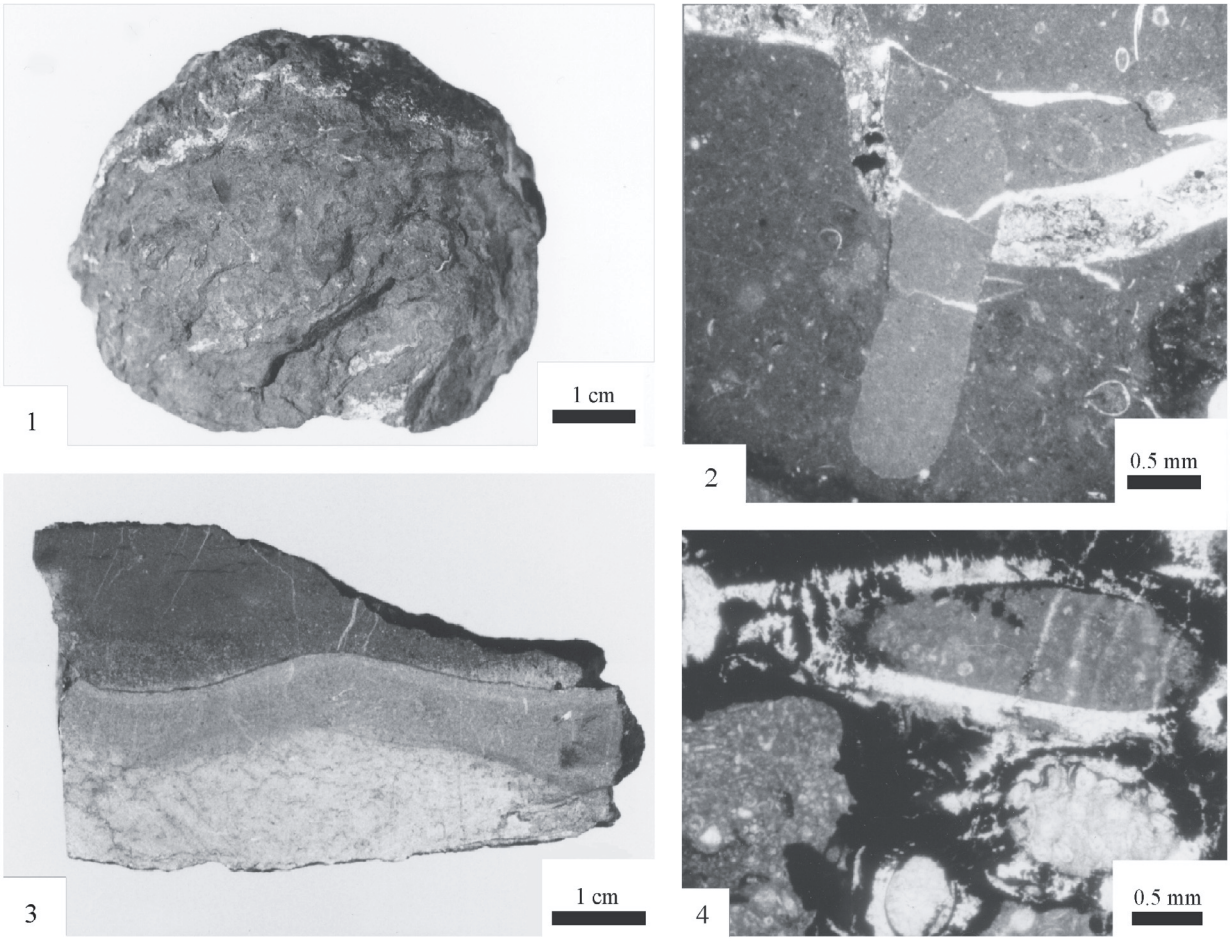

Fig. 4. 1 — Manganese nodule. Chtelnica, sample Cht1. **2** — Aragonite shell of ammonite (white) was dissolved shortly after the deposition and the mold was filled with micrite containing small bioclasts. Hardground was formed as a result of rapid lithification and then perforated by a boring organism. The boring was filled with grey, pure micrite. Chtelnica, transmitted light, parallel polars. **3** — Manganese crust (black, top) overlying Fe crust (light grey). Hrušové, sample Hru1, polished slab. **4** — Detail of the serpulid microreef, colonizing the hardground. The serpulid tubes are affected by microborings and impregnated by Mn-oxides. Vršatec, transmitted light, parallel polars.

Mikušovce

The locality near Mikušovce was recently described by Mišík & Rojkovič (2002). An abandoned, collapsed mine gallery occurs SW of Mikušovce village (Za Skalkou locality), at the altitude 420 m above sea-level. According to Andrusov et al. (1955), this is the so-called Upper Deposit. High-grade manganese ore is found at the entrance to the gallery, filling a cleft in the Middle Jurassic crinoidal limestones. The cleft is oriented 110–115°/60° towards NNE. The thickness of the massive ore is about 10–30 cm. East of the gallery, about 100–300 m west of a local creek, is the mine waste dump. In limestone material, manganese ore can be found locally, mainly along the southern margin of the dump.

The base of the klippe at the mine gallery is formed by spotty limestone and marlstone (Aalenian — "Opalinum" Beds), overlain by crinoidal limestone (Smolegowa and Krupianka Formation — Bajocian–Bathonian) and red nodular to massive micritic limestone (Czorsztyn Limestone — Callovian–Oxfordian). In this micritic limestone, lenses of manganese ores are developed. The Malm is represented by pale massive bioherm limestone (Vršatec Limestone).

Vršatec

The locality occurs in the part of the Vršatec Klippen (Czorsztyn Unit) north of the road cutting the Vršatec Saddle, about 600 m SW from the elevation point 898 m (Javorník Hill). The locality was studied in detail by Aubrecht et al. (2000). A black manganese crust (hardground) and oncoids occur in a position which is not yet clear. The thickness of the crust varies from 15 to 40 cm but its lateral extension is covered by debris and vegetation. Below the hardground there are pale crinoidal limestones of Bajocian–?Bathonian age; the overlying strata are problematic. There is red mudstone, most probably Upper Jurassic, with layers of crinoidal limestone. Microfacies analysis shows that they represent biomicrites with planktonic crinoids *Saccocoma*, crinoidal ossicles, *Globochaete alpina*, foraminifers *Lenticulina* sp., ostracods, dinocysts and common lithoclasts. The only stratigraphically valuable microfossil is *Saccocoma* indicating most likely a Kimmeridgian to Early Tithonian age. The ammonite fauna indicate that the time span of the hardground formation is Oxfordian to Lower Tithonian. The hardground comprises encrusting foraminifers *Bullopora tuberculata* and serpulids

(Fig. 4.4). The manganese crust is commonly penetrated by ptygmatitically folded calcite veinlets that testify an initial plasticity of the manganese crust. Hedbergelid foraminifers likely to be of Albian age occur in tiny lenses of microbreccia within the hardground. Their presence may be explained by occurrence in the filling of younger neptunian microdykes.

Methods

Minerals were studied by polarizing microscope in both transmitted and in reflected light and by scanning electron microscope (SEM). They were analysed by wave-dispersion X-ray microanalysis (WDX) and by X-ray diffraction analysis (XRD). WDX analyses of Al, Ba, Ca, Fe, K, Mg, Mn, Na, Si and Sr were carried out on a JEOL-733 Superprobe X-ray microprobe (Geological Survey of the Slovak Republic). Natural and synthetic standards were used to calibrate the systems: Al_2O_3, $BaSO_4$, wollastonite, rhodonite, hematite, orthoclase, MgO, albite, SiO_2 and $SrTiO_3$. Electron beam was stabilized at 15–18 nA, with 15 and 20 kV accelerating voltage. Counts were acquired for 100 seconds, and recalculated using XPP quantitative correction. The electron beam was focused on 2–5 micrometers. Detection limits were better than 0.1 wt. %. Relative standard deviation ranged from ±5 % (for 1 wt. %) to ±25 % (for 0.1 wt. %). Chemical composition was calculated using the Minfile programme.

X-ray diffraction (XRD) analyses were done on a Philips PW 1710 diffractometer. Samples with high content of Fe were analysed by CoK_α radiation ($\lambda\alpha_1 = 1.78896\times10^{-10}$ m, $\lambda\alpha_2 = 1.79285\times10^{-10}$ m), and CuK_α radiation ($\lambda\alpha_1 = 1.54060\times10^{-10}$ m, $\lambda\alpha_2 = 1.54439\times10^{-10}$ m) was used in the case of other samples. Accelerating voltage of 35 kV and beam current of 20 mA were used in the range 4 to 60° 2Θ, with shift 0.02° 2Θ.

Chemical composition of rocks was determined by X-ray fluorescence analysis (XFA) for major elements of the rocks, and by colorimetry for P_2O_5. Major elements were analysed on the X-ray spectrometer Philips PW 1410/20. Instrumental conditions: X-ray tube with Rh anode (voltage 40 kV, current 40 mA), gas flow detector with Ar/CH_4 = 90/10 filling, crystal LiF 200 for Fe, Mn, Ti, Ca, K and TlAP for Si, Al, Mg, Na. Samples (1.3 g) were fused with $Li_2B_4O_7$ (5.5 g) at 1050 °C in Pt-crucible. The accuracy of the analyses with respect to the certified values of the standard materials is within ±20 % for light elements (Na, Mg) and Mn and ±5–10 % for other elements. Rare earth elements (REE) were analysed by atomic emission spectroscopy with inductively coupled plasma (AES-ICP). Samples sintered with Na_2O_2 were dissolved by HCl and later by oxalic acid. Samples were analysed by sequential atomic emission spectrometer with inductively coupled plasma Liberty 200 VARIAN with ultrasonic nebulizer CETAC. Detection limits ranged from 0.03 to 1 ppm. Relative standard deviation ranged from ±3 % (for 0.1 wt. %) to ±20 % (for 0.001 wt. %). Optical emission spectroscopy (OES) was used for B, Ba, Co, Cr, Cu, Ni, Pb, Sr and V. The spectra of samples were recorded by the grid spectrograph PGS-2 in UV and visual area, with 6 A power arch as activating source. Measuring time was 90 s. Rock-Eval pyrolysis was used to determine organic carbon (TOC) content.

Results

Manganese mineralization

Pyrolusite, "psilomelane" and wad were described mostly as manganese minerals of oxidic ore in limestone (Andrusov et al. 1955). This study has confirmed that pyrolusite is accompanied by romanèchite, manganite and todorokite. Iron hydroxides dominate in the brown coloured part of hardgrounds.

Pyrolusite β-MnO_2 is an abundant mineral in the studied ores. It can be distinguished from other manganese minerals by its characteristic yellow tint and high reflectivity. Columnar crystals are from several micrometers to 0.01 mm, up to 0.05 mm long. Larger grains can be seen along the fissures in fine-grained pyrolusite. They form zoned colloform botryoidal to concentric aggregates (about 0.1 mm across) or radial aggregates about 0.1 mm up to 3 mm across. Pyrolusite replaces spheroidal foraminifers (Fig. 5.1), bivalves, echinoderm fragments and ammonites. Columnar microstromatolites (up to 0.5 mm long and 0.1 mm thick) are often replaced by pyrolusite in manganese crusts. Manganese nodules are formed by zoned aggregates of pyrolusite up to 0.5 mm thick. Pyrolusite also fills traces after fossils (up to 1 cm thick). Thin zones of pyrolusite (about 0.05 mm thick) are often alternating with romanèchite and calcite. It replaces, or cuts in thin veinlets, calcite, romanèchite, manganite and todorokite. Microscopic identification of pyrolusite is consistent with the WDX chemical composition (Table 1) and the XRD data.

Romanèchite $(Ba,H_2O)_2(Mn^{++++},Mn^{+++})_5O_{10}$ is a common mineral in the hardgrounds. Colloform zoned aggregates (0.1 to 1.5 mm across) consist of irregular grains (0.01 to 0.05 mm in size) or needle shaped crystals (up to 0.01 mm long) in the central part forming a radial texture. Thin zones (up to

Table 1: Chemical composition of pyrolusite (wt. % of oxides and atomic proportion of elements O = 2).

No	Sample	MnO_2	Fe_2O_3	SiO_2	CaO	Total
1	Hr1	98.0	1.6	0.3	0.6	100.5
2	Hr1	99.0	1.4	0.3	0.4	101.1
3	Hr1	96.3	0.9	0.5	0.5	98.1
4	Hr1	96.9	1.3	0.3	0.8	99.2
5	HS1	94.6	2.9	0.7	0.8	99.1
6	HS1	94.4	3.4	0.9	0.9	99.6
7	HS1	95.7	3.6	0.7	0.7	100.8
8	HS1	92.2	2.8	1.0	0.8	96.7
9	Vrš1	92.1	2.1	2.3	0.5	97.0
10	Vrš1	92.0	2.5	2.0	0.6	97.1
No	**Sample**	**Mn**	**Fe**	**Si**	**Ca**	**Total**
1	Hr1	0.978	0.018	0.004	0.009	1.009
2	Hr1	0.981	0.016	0.004	0.007	1.007
3	Hr1	0.982	0.010	0.007	0.007	1.006
4	Hr1	0.979	0.014	0.004	0.012	1.009
5	HS1	0.959	0.032	0.010	0.013	1.015
6	HS1	0.952	0.037	0.013	0.014	1.017
7	HS1	0.954	0.040	0.011	0.011	1.016
8	HS1	0.955	0.032	0.014	0.013	1.014
9	Vrš1	0.944	0.024	0.034	0.009	1.010
10	Vrš1	0.944	0.028	0.030	0.010	1.012

Localities (for all tables): Bo — Bolešov, Bz — Bzince pod Javorinou, Hru — Hrušové, HS — Horné Sŕnie, Ch — Chtelnica, and Vrš — Vršatec.

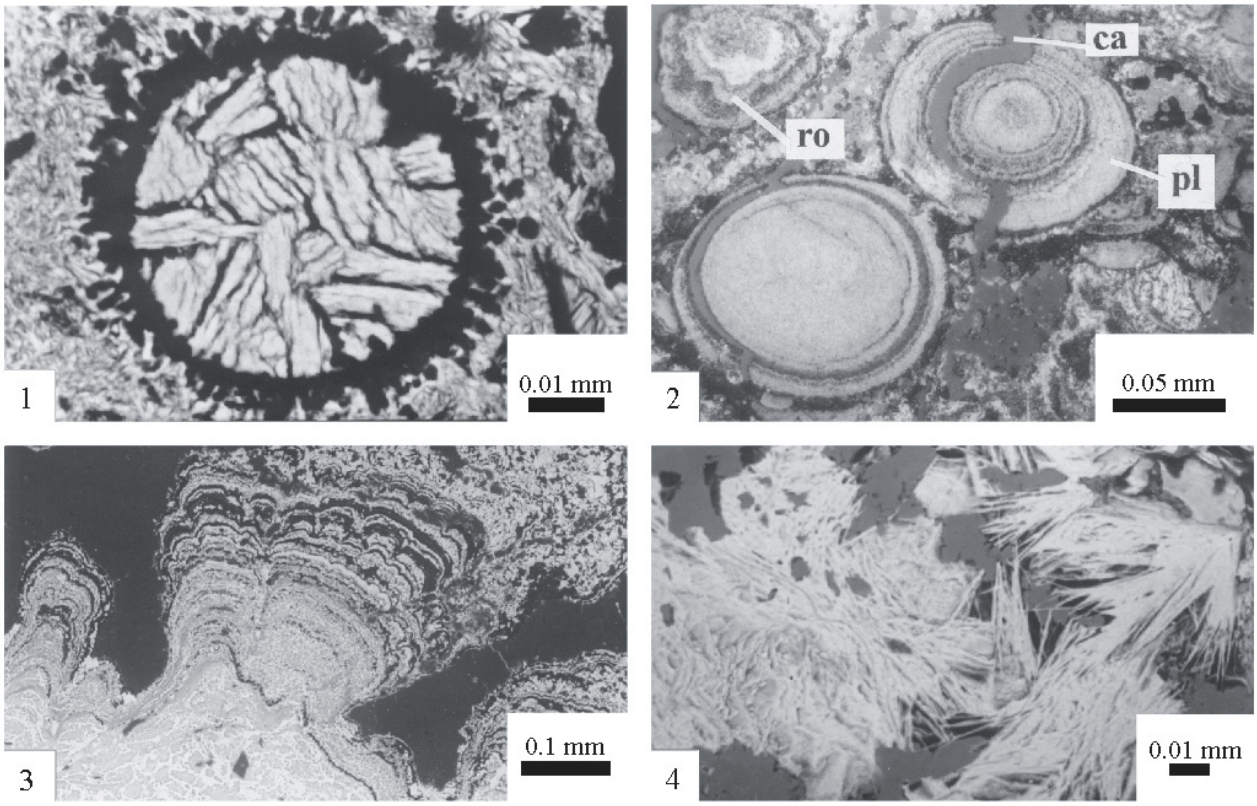

Fig. 5. 1 — Spheroidal aggregate of coarser pyrolusite replacing foraminifers in fine-grained pyrolusite. Hrušové, sample Hr1, SEM-BEI. **2** — Colloform zoned aggregates of pyrolusite (pl) and romanèchite (ro) are cut by veinlets of younger calcite (ca). Vršatec, sample Vrš6, reflected light, parallel polars. **3** — Colloform zonal aggregates of todorokite (light grey) replacing columnar stromatolites. Horné Sŕnie, sample HS1, SEM-BEI. **4** — Aggregate of todorokite (white) in limestone. Hrušové, sample Hru3a, SEM-BEI.

0.1 mm) are alternated with pyrolusite (Fig. 5.2). Romanèchite is easily distinguished by back-scattered electron image in scanning electron microscope (BEI-SEM) as a lighter phase due to increased content of Ba, as was confirmed by WDX analysis (Table 2).

Todorokite $(Mn^{+2},Ca,Mg)Mn^{+4}{}_3O_7 \cdot H_2O$ is abundant in some localities. Colloform aggregates are concentric or they form crusts up to 1 cm thick with columnar microstromatolites on their surface (Fig. 5.3). Zoning, as well as radial texture, can be observed in aggregates. Aggregates consist of xenomorphic grains (0.01 to 0.05 mm in size). Needle–like crystals form radial aggregates or bundles (Fig. 5.4). Todorokite completely replaces fossils (foraminifers). It forms dark cores of concentric aggregates (up to 0.03 mm across) rimmed with romanèchite. CaO content ranges from 4.5 to 8.6 wt. % (Table 3). Chemical composition is close to todorokite or ranciéite $(Ca,Mn^{++})Mn^{++++}{}_4O_9 \cdot 3(H_2O)$. Ranciéite was identified in Bolešov by XRD (Aubrecht et al. 1998). Todorokite was also confirmed by XRD.

Manganite γ-MnOOH was found in the continental limestone breccia of the Early Cretaceous age. Spherical, radial and fan-like aggregates up to 3 mm in size replace non-marine algae. The central part of the aggregates formed by xenomorphic grains is overgrown by alternating zones of calcite, romanèchite and manganite with radial texture. Manganite is replaced and cut by veinlets of pyrolusite. Identification of manganite was confirmed by XRD and WDX in remobilized supergene ore in Lednica and Mikušovce (Mišík & Rojkovič 2002).

Table 2: Chemical composition of romanèchite (wt. % of oxides and atomic proportion of elements O = 10).

No	Sample	MnO_2	Fe_2O_3	MgO	SiO_2	K_2O	CaO	BaO	Total
1	Bz1	77.5	0.0	1.2	0.2	0.4	2.6	3.9	85.6
2	Bz1	76.5	1.2	1.4	0.1	0.5	2.6	4.3	86.7
3	Bz1	77.2	1.1	1.2	0.2	0.5	2.4	4.4	87.0
4	Hru3	73.5	2.2	0.3	0.4	0.5	3.3	7.8	88.0
5	Vrš2	74.5	3.3	0.0	1.7	2.0	0.6	8.5	90.5
6	Vrš2	76.1	3.6	0.0	0.4	2.0	0.6	8.1	90.8
7	Vrš2	76.0	3.8	0.0	1.8	2.0	0.6	8.2	92.5
8	Vrš2	77.5	4.0	0.0	0.6	2.0	0.6	8.1	92.8
9	Vrš6.1	79.1	3.3	0.0	2.2	2.5	0.3	4.8	92.2
10	Vrš6.2	76.1	2.8	0.0	2.2	2.4	0.3	5.3	89.2
No	**Sample**	Mn^{+4}	Fe^{+3}	**Mg**	**Si**	**K**	**Ca**	**Ba**	**Total**
1	Bz1	4.712	0.000	0.154	0.014	0.040	0.240	0.134	5.294
2	Bz1	4.629	0.082	0.177	0.009	0.058	0.247	0.149	5.350
3	Bz1	4.650	0.075	0.155	0.015	0.054	0.225	0.152	5.325
4	Hru3	4.568	0.145	0.039	0.033	0.051	0.318	0.273	5.427
5	Vrš2	4.469	0.215	0.000	0.143	0.221	0.055	0.288	5.391
6	Vrš2	4.611	0.238	0.000	0.040	0.224	0.057	0.279	5.449
7	Vrš2	4.448	0.240	0.000	0.156	0.216	0.053	0.273	5.385
8	Vrš2	4.589	0.261	0.000	0.048	0.219	0.052	0.272	5.440
9	Vrš6.1	4.503	0.203	0.000	0.179	0.258	0.027	0.156	5.339
10	Vrš6.2	4.507	0.181	0.000	0.186	0.266	0.031	0.178	5.349

Goethite α-FeOOH and other iron-hydroxides form crusts and aggregates disseminated in limestone. Crust of manganese minerals is overgrown by brown and yellow crust of iron

Table 3: Chemical composition of todorokite (wt. % of oxides and atomic proportion of elements O = 7).

No	Sample	MnO_2	Fe_2O_3	MgO	SiO_2	K_2O	CaO	BaO	Total
1	Bo1	78.0	0.0	0.0	0.1	0.4	8.4	0.0	86.9
2	Bo1	77.6	0.0	0.0	0.2	0.3	8.6	0.0	86.7
3	HS1	83.0	0.4	0.5	0.2	1.2	5.1	0.0	90.4
4	HS1	82.3	0.6	0.5	0.3	1.2	4.9	0.0	89.8
5	HS1	80.0	2.5	0.0	0.6	1.1	4.5	0.0	88.7
No	**Sample**	**Mn^{+4}**	**Fe^{+3}**	**Mg**	**Si**	**K**	**Ca**	**Ba**	**Total**
1	Bo1	3.218	0.000	0.000	0.006	0.031	0.537	0.000	3.792
2	Bo1	3.207	0.000	0.000	0.012	0.023	0.551	0.000	3.793
3	HS1	3.277	0.017	0.043	0.011	0.087	0.312	0.000	3.747
4	HS1	3.269	0.026	0.043	0.017	0.088	0.302	0.000	3.745
5	HS1	3.222	0.110	0.000	0.035	0.082	0.281	0.000	3.729

hydroxides. Thin zones of iron hydroxides alternate with manganese minerals and calcite in the Mn-Fe nodules. Goethite also forms veinlets in todorokite and pyrolusite. Their heterogeneity is documented by back-scattered electron image in scanning electron microscope (BEI-SEM), and WDX confirmed several wt. % of MnO_2, Al_2O_3 and SiO_2.

Calcite $CaCO_3$ is a dominant mineral of limestone. It is fine-grained in biomicritic limestone cementing fossils (foraminifers, bivalves, echinoderms and ammonites). Coarser grained calcite (grains up to 0.7 mm) replaces fossils and forms veinlets. Younger calcite veinlets cut biomicritic limestone as well as the aggregates of manganese minerals. Cores of the manganese nodules are formed by limestone with coarse calcite crystals (up to 1 mm), and by fossils. The cores coated by alternating zones of calcite, pyrolusite and iron hydroxides are up to 0.1 mm thick. Syneresis fissures in nodules are filled with coarser grained calcite. WDX has confirmed up to 0.6 wt. % of MgO and FeO.

Geochemical characteristics of manganese ore

Typical crusts and nodules with abundant iron hydroxides (Horné Sŕnie, Chtelnica and Vršatec) show distinctly increased iron content (Table 4). Manganese content in the ore increases with increasing ratio of supergene pyrolusite (Bolešov, Hrušové), especially in places of supergene mobilization and accumulation, where the highest Mn/Fe ratio is noted (Mikušovce, Lednica, Mišík & Rojkovič 2002). The highest content of Mn was found in fissures and cavities of manganese ore in Mikušovce and Lednica, reaching up to 48 wt. %, with higher Mn/Fe (Nx10) comparing to sedimentary manganese mineralization in the Callovian-Oxfordian red limestone, with low Mn/Fe ratio (Nx1). Si/Al ratio in average corresponds to 1.84 (Fig. 6).

Ba, Co, Cu and Ni are accompanying trace elements of manganese mineralization. Presence of romanèchite increases Ba content over 2000 ppm. Co, Cu and Ni are dominant trace elements in the studied manganese crusts and nodules. The total Ni+Co+Cu content in the studied samples reaches up to 0.5 wt. % with maximum values for Ni > 2000 ppm, Cu > 3000 ppm and Co over 850 ppm (Fig. 7). Ni shows a positive correlation with Fe and negative with Mn. Co shows positive correlation with Mn. Increased content of Pb and V suggests that the elements are bound to iron hydroxides. Sr is associated with carbonates. The content of organic carbon is low (average content 0.20 wt. %). REE distribution shows only slight dominance of light REE (LREE), and distinct positive Ce anomaly (Table 5, Fig. 8).

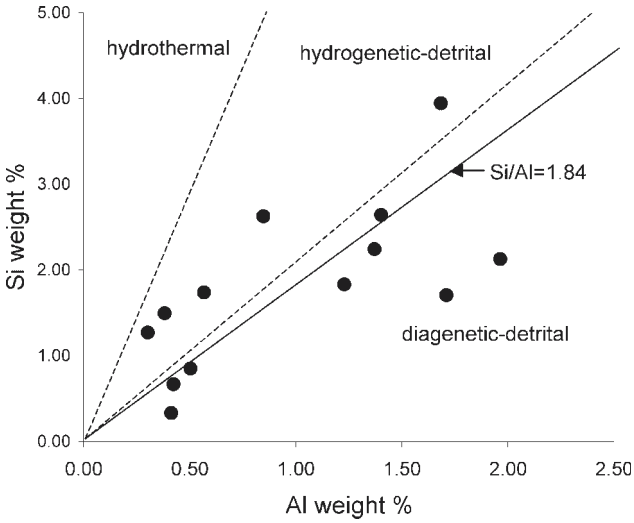

Fig. 6. Si/Al plot in the studied manganese ore and limestone.

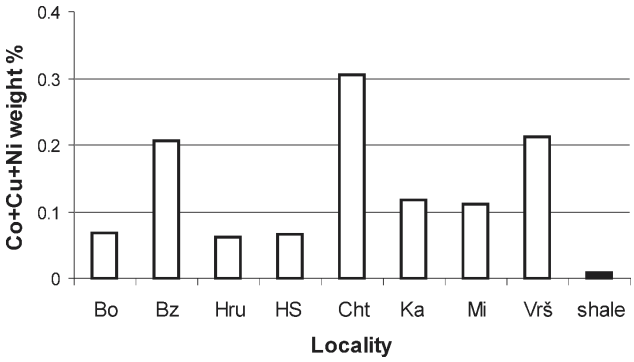

Fig. 7. Contents of Co+Cu+Ni in: Bo — Bolešov, Bz — Bzince pod Javorinou, Hru — Hrušové, HS — Horné Sŕnie, Cht — Chtelnica, Ka — Kamenica, Mi — Mikušovce and Vrš — Vršatec compared to average content in Jurassic shale (shale).

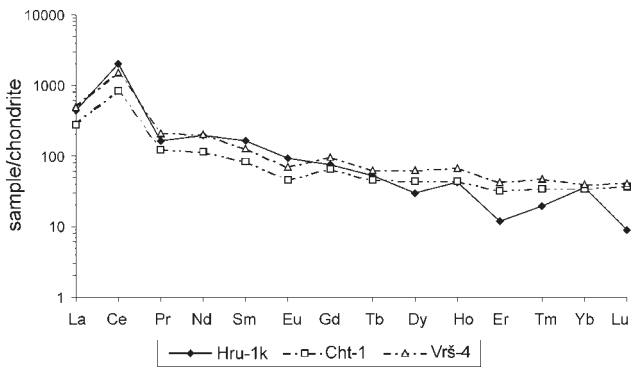

Fig. 8. REE distribution in the studied manganese hardgrounds (Hru-1k — Hrušové, Cht-1 — Chtelnica and Vrš-4 — Vršatec).

Table 4: Chemical composition of manganese ores and limestones.

Sample	Bo1	Bo2	Bz1	Hru1a	Hru1k	Hru2	HS1	Cht1	Cht5	Ja1	Ka1	Vrš1	Vrš4
SiO_2	1.82	3.92	3.65	3.20	5.62	2.72	1.43	5.65	4.80	3.72	8.44	4.55	0.71
Al_2O_3	0.95	2.32	3.23	0.72	1.60	0.57	0.80	2.65	2.59	1.07	3.18	3.71	0.78
FeO	0.09							1.47				0.12	
Fe_2O_3*	0.63	5.19	28.98	4.55	3.18	7.85	1.86	10.99	10.76	0.73	2.12	11.03	9.31
MnO	48.08	9.15	3.31	0.41	43.68	0.88	4.97	14.23	23.25	1.41	3.17	12.21	12.61
MgO	1.36	2.31	0.90	0.44	0.05	0.58	0.45	0.81	0.78	0.61	0.92	1.49	0.52
CaO	23.69	43.11	30.73	51.47	23.96	50.33	49.87	34.08	31.07	52.98	45.47	35.19	44.38
Na_2O	0.21	0.20	0.11	0.01	0.20	0.05	0.13	0.03	0.09	0.13	0.10	0.10	0.06
K_2O	0.10	1.06	0.32	0.25	0.37	0.63	0.32	0.70	0.96	0.76	2.22	0.76	0.39
TiO_2	0.09	0.11	0.12	0.04	0.14	0.05	0.06	0.29	0.24	0.05	0.13	0.25	0.15
H_2O-	0.25	0.48	0.61	0.04	0.44	0.04	0.28	0.43	0.44	0.16	0.40	0.19	0.06
LOI	22.25	31.54	27.68	38.57	20.44	35.94	39.52	28.13	24.51	37.88	33.42	30.08	30.80
P_2O_5	0.14		0.71	0.20	0.19		0.21	0.33	0.16	0.16	0.10	0.79	
Total	99.66	99.38	100.35	99.92	99.87	99.64	99.90	99.80	99.66	99.66	99.66	100.48	99.76
B	19	25	154	26	107	21	17	69	79	16	32	55	27
Ba	132	40	92	51	2127	73	222	448	1189	938	630	3100	>3000
Co	155	449	424	46	498	70	177	491	343	19	155	861	362
Cr	4	<3	34	3	2	3	2	9	10	8	9	4	<3
Cu	93	18	300	38	657	40	77	>3000	412	17	269	452	126
Ni	264	400	1342	119	300	114	396	980	881	48	758	2019	446
Pb	39	171	131	64	1100	101	173	187	232	52	50	669	615
Sr	182	271	56	113	244	106	270	252	292	391	105	412	>500
V	28	62	337	38	91	24	34	148	130	32	110	211	148
TC%	11.33	8.65	2.73	11.08	3.98	10.87	10.70	6.53	6.02	9.78	8.26	7.20	9.05
TOC%	0.96	0.08	traces	0.98	0.07	0.10	0.07	0.18	traces	traces	0.10	traces	0.12
TIC%	10.37	8.57	2.73	10.1	3.91	10.77	10.63	6.53	6.02	9.78	8.16	7.20	8.93

Locality: Bo — Bolešov, Bz — Bzince pod Javorinou, Hru — Hrušové, HS — Horné Srnie, Cht — Chtelnica, Ja — Jarabina, Ka — Kamenica, and Vrš — Vršatec. Fe_2O_3* — total iron if FeO is missing.

Table 5: REE in manganese ore (in ppm).

	MnHru-1k	MnCht-1	MnVrš-4
La	108.00	68.00	122.00
Ce	1295.00	526.00	960.00
Pr	16.00	12.00	20.00
Nd	93.00	54.00	96.00
Sm	25.00	13.00	20.00
Eu	5.50	2.70	4.00
Gd	15.60	13.50	19.90
Tb	2.00	1.70	2.40
Dy	7.60	11.10	15.90
Ho	2.40	2.50	3.90
Er	2.00	5.40	7.10
Tm	0.50	0.90	1.20
Yb	5.90	5.80	6.60
Lu	0.23	0.95	1.03

Discussion

The Jurassic manganese crusts and nodules mostly correspond to the recent submarine hardgrounds. They were mostly formed on seamounts or other isolated places with low sedimentation rates, and they show association of bacterial stromatolites and sessile foraminifers (Jenkyns 1970; Roy 1980; Ballarini et al. 1994; Dromart et al. 1994). Manganese crusts accumulate on submarine seamounts and plateaus at depths >1000 m where bottom currents prevent sediment accumulation and growth occurs mainly at the sediment/water interface (Glasby 2000).

There are three principal modes of formation of the manganese crusts and nodules: hydrogenetic, diagenetic and hydrothermal. *Hydrogenetic* deposits form directly from seawater in an oxidizing environment (Glasby 2000). They are characterized by slow growth (about 2 mm $10^6 yr^{-1}$) (Glasby 2000). The hydrogenetic nodules were formed by precipitation from the sea-water (with possible bacterial mediation) and their growth also comprehends early diagenetic formation (Bonatti et al. 1972).

A colloid-chemical model for the hydrogenetic precipitation of ferromanganese crusts on seamounts was proposed (Koschinsky & Halbach 1995). However "… the types of reactions that occur in the water column and at the precipitation surface are poorly known." (Hein et al. 1997). In the first stage Mn^{2+}-rich water from the oxygen minimum zone is mixed with oxygen-rich deep-water, and oxidized Mn(IV) and other metals like Fe, Ti, Al, and Si form oxide and hydroxide colloids phase (Koschinsky & Halbach 1995). These form mixed colloidal phases and scavenage trace metals by sorptive processes which are dominated by coulombic and chemical interactions between colloidal surfaces and dissolved metal species phase (Koschinsky & Halbach 1995). Co, Ni and Cu are present in seawater mainly as hydrated and labile complexed cations phase (Koschinsky & Halbach 1995). The manganese colloidal phases scavenge these hydrated cations via adsorption to the negatively charged surface of manganese oxides and anions (Hein et al. 1997). Elements forming carbonate and hydroxide complexes and oxyanions in seawater like Pb, Mo, V are bound to the slightly positive charge of the iron hydroxide surfaces (Koschinsky & Halbach 1995; Hein et al. 1997). Ti mainly forms a hydrogenetic phase, probably consisting of $TiO_2 \cdot 2H_2O$ intergrown with the amorphous FeOOH phase (Koschinsky & Halbach 1995). In the second stage, the colloidal phases precipitate on the substrate rocks of the seamounts as ferromanganese oxide encrustations, incorporating the sorbed heavy metals into the mineral phases (Koschinsky & Halbach 1995).

Diagenetic deposits result from diagenetic processes within the underlying sediments leading to upward supply of elements from the sediment column and they are characterized by faster growth rates (10–100 mm $10^6 yr^{-1}$, Glasby 2000). Metals supplied by upward diffusion from deeper reducing parts of sediments are precipitated close to the sediment/water interface. Transport of metal in the ionic form (e.g. Mn^{2+}, Ni^{2+}, Cu^{2+}, Zn^{2+}) is typical for early-diagenetic growth (Halbach et al. 1981). The intensity of early diagenetic processes depends on the sufficiency of organic matter or on the biological productivity in the water column (Halbach et al. 1981). Surficial diagenesis is a significant source of metals to manganese nodules in siliceous ooze areas, where metals are supplied by organic matter through the water column and release of metals at the seafloor (Müller et al. 1988).

Hydrothermal deposits precipitate directly from hydrothermal solutions in areas with high heat flow such as mid-ocean ridges, back-arc basins and hot spot volcanoes (Glasby 2000). They are characterized by high to extremely high growth rates (>1000 mm $10^6 yr^{-1}$) and low, to very low trace element contents (Glasby 2000). They tend to be associated with hydrothermal sulphide deposits and iron oxihydroxide crusts (Glasby 2000). The important source of manganese in the pelagic environment is often related to hydrothermal activity associated with global tectonic processes (Corbin et al. 2000). Volcano-sedimentary manganese deposits associated with cherts are closely related to juvenile solutions of basalts. For example, the sediments with Fe accumulation of submarine hydrothermal origin in the Tyrrhenian Sea contain 12.2 to 45 % of Fe and low contents of Mn, Cu, Zn, Ni and Co, suggesting hydrothermal origin (Savelli et al. 1999).

The chemical composition of the Tethyan Jurassic nodules with fine lamination of Fe-Mn oxides is variable and, similarly, crusts (2 to 5 mm rarely up to 2 cm thick) show changing Mn/Fe ratios (Cronan et al. 1999). The colloidal chemical model enables us to compare the chemical composition of the studied manganese crusts and nodules with data from cores and nodules of the recent oceans. Manganese nodules in the Pacific Ocean have been formed as a result of diagenetic growth from pore waters, or by hydrogenetic growth from bottom waters (Halbach et al. 1981). Fe-poor todorokite is typical for early diagenetic nodules, while α-MnO_2, intergrown with $FeOOH \cdot H_2O$, is formed by hydrogenetic growth (Halbach et al. 1981).

Zoned alternation of the studied manganese oxides and hydroxides with iron hydroxides and calcite is dominant and indicates hydrogenetic accumulation of Fe-Mn hydroxides and oxides in the crusts and nodules. Fe-Mn crusts that occur on most seamounts in the ocean basins have a mean Fe-Mn ratio of 0.7 for open ocean seamount crusts and 1.2 for continental margin seamont crusts (Hein et al. 1997). The Fe/Mn ratio in the studied manganese crusts and nodules range from 0.3 to 0.8. Hydrothermal manganese crusts in the recent oceans are characterized by high Mn/Fe ratios (from 10 to 4670 — Glasby 2000). Increased content of Fe, Co, Ti and Mn/Fe ratios lower than 2.5 are typical for hydrogenetic nodules (Halbach et al. 1981). The studied hardgrounds and nodules show Mn/Fe ratios from 1 to 4. This ratio is distinctly higher in a younger supergene mineralization, where Mn/Fe = 32 (Mišík & Rojkovič 2002). The high-grade manganese ores, with high Mn/Fe ratio, correspond to supergene accumulation.

Manganese nodules formed in oxic environments are enriched in Ni, Co, Cu and other elements. The presumed source of Co, Ni and Cu in manganese ores are weathered mafic and ultramafic rocks on land (Fan et al. 1999). The average content of the elements in manganese nodules varies in the range of 11–14 % Mn, 6.2–20 % Fe, 0.16–1.1 % Ni, 0.17–1.8 % Cu, 0.01–0.7 % Co, and 0.05–0.25 % Pb (Schweisfurth 1971). Ni, Mo, Cu, Co and Zn are bound to Mn, whereas Ti, V and Cr are associated with Fe (Goodell et al. 1971). The diagenetic nodules rich in Ni and Cu are concentrated in deeper parts of the sea, below zones of weak to moderate biological activity (Halbach et al. 1981). Hydrothermal manganese crusts in the recent oceans are characterized by low contents of Cu (20 to 1000), Ni (1 to 1403), Zn (1 to 1233), Co (6 to 209) Pb (0 to 93 ppm) and detrital silicate minerals (Glasby 2000).

The increased contents of Ni, Co, Cu, as well as Fe/Mn and Si/Al ratios in the studied samples indicate the hydrogenetic to diagenetic origin of the studied ores (Figs. 6, 7).

Ce distribution is closely linked to the redox cycling of manganese (Palumbo et al. 2001). Chondrite-normalized REE patterns generally show a positive Ce anomaly and abundant ΣREE for hydrogenetic and mixed hydrogenetic-diagenetic deposits, whereas the Ce anomaly is negative for hydrothermal deposits and ΣREE contents are low (Matsumoto et al. 1985; Hein et al. 1997; Usui et al. 1997; Kuhn et al. 1998). Positive Ce anomalies in the distribution patterns reveal preferential uptake of Ce especially in normal hydrogenetic crusts (Kuhn et al. 1998). Oxidative uptake of Ce and Co by fast sinking large biogenic particles can more effectively convey nutrient-type metals involved with them to the sea floor because of their shorter residence time in oxic water (Ohta et al. 1999). Ce/La ratios of the nodules can be used as redox indicators to trace the oxygen content of the ambient water mass and the flow path (Kasten et al. 1998).

REE distribution in the studied manganese crusts with slightly dominant LREE and distinct positive Ce anomaly corresponds to hydrogenetic to diagenetic origin and it does not indicate the presence of a volcanic source for the formation of the studied manganese mineralization (Fig. 8). Moreover, Jurassic volcanic rocks have not been found in the studied area and distant volcanism in the Meliata Ocean had a mafic to ultramafic character with different REE distribution. Hydrothermal crust La/Ce ratios are similar to sea water La/Ce ratio 2.8 and all other deposits are enriched in Ce relative to sea-water approaching an apparent lower limit of La/Ce ~0.25 (Toth 1980). La/Ce ratios in our samples ranging from 0.08 to 0.13 are very different from crusts of hydrothermal origin which are close to ratio 2.8 of the sea-water.

The average content of organic carbon in deep ocean nodules is 0.17 %, while on the continental shelf forms it is about 2.1 % (Manheim 1965). The average organic carbon content in the studied samples is 0.20 wt. %.

Association of the studied manganese mineralization with microstromatolites is distinct and we have to take into account a role of microorganisms in manganese deposition. Present-day submarine “hardgrounds” are developed in places of pe-

lagic and hemipelagic oozes (cf. hardground near Barbados, Roy 1980). Encrusting bryozoa and worm tubes at the surface and foraminifers, sponge spicules and manganiferous nodules with corals, coccoliths and calcareous serpulid tubes have been reported from the Pacific Ocean (Roy 1980).

Various living or dead microorganisms as bacteria, algae, mosses, fungi etc. played a particularly great ore-generating role in the formation of ancient deposits of manganese. Their geochemical activities, including transporting action were associated with the physiologícal processes of manganese extraction from solutions, its oxidation and concentration in, and around, plant cells (Serdyuchenko 1980). Some microorganisms corresponding to ultra-microfossils reported by Zhang et al. (1997) can also be considered as constructors of the pelagic manganese nodules. Mn^{+4} is probably the primary product of bacterial Mn^{+2} oxidation spores of the marine *Bacillus* (Bargar et al. 2000). The microbes change the conditions of oxidation and reduction in the system, and their effect on the element precipitation is much stronger than the chemical actions and accelerates the enrichment of Fe and Mn (Yan et al. 1999). After the death of the microbes, their bodies are accumulated on the sediment/seawater interface and form polymetallic nodules. On the walls of some mineralized microbial cells there are sheaths of Fe and Mn oxides (Yan et al. 1999). Microbial Mn oxidation is a ubiquitous process in oxygenated marine environments (Moffett 1997). Diagenetic ferromanganese nodules in an oxic deep-sea sedimentary environment grew from remobilized metal ions as well as reprecipitated Mn-oxide grains, which were supplied to the nodules episodically during the stirring of bottom sediments by benthic fauna and intermittent strong bottom current flow (Jung & Lee 1999). Post-depositional modifications of the nodules can be controlled by accreted biogenic remains as indicated by their progressive dissolution with increasing depth from nodule surfaces, their pseudomorphic replacement by todorokite and the later growth of phillipsite and todorokite in the microfossil molds (Banerjee et al. 1999).

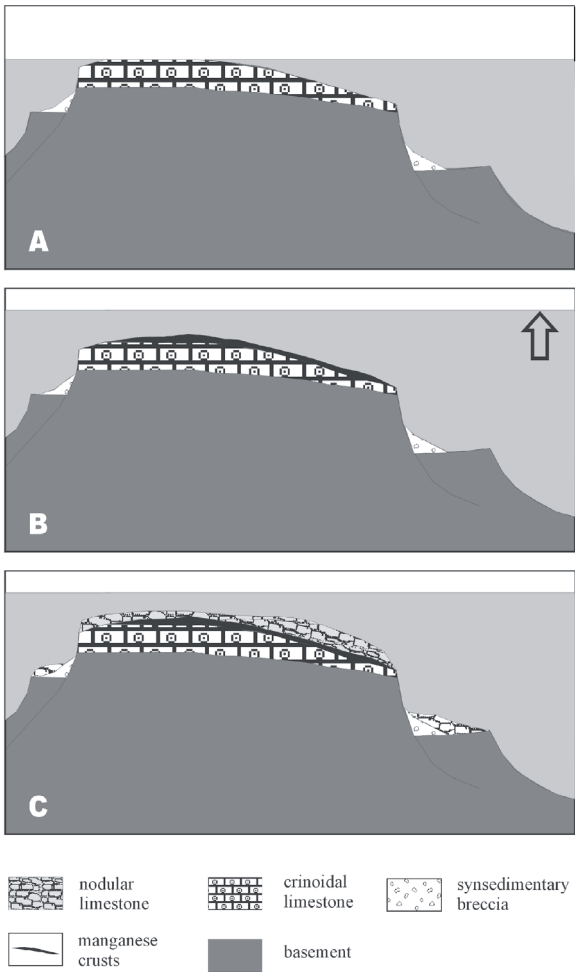

Fig. 9. Model of Jurassic manganese hardground formation in a transgressive oceanic regime. A rapid sea-level rise resulted in drowning of the shallow-water carbonate platform and in succeeding starvation of the sedimentary area. The latter, together with bottom currents with increased CO_2 contents resulted in formation of omission surfaces and hardgrounds. A condensed sedimentation of Ammonitico Rosso limestones followed afterwards.

The manganese hardgrounds of small extent examined in this study, occurring in the Pieniny Klippen Belt (mainly at the base of the Czorzstyn Limestone), represent sediments of pelagic up to shallow neritic marine facies (Fig. 9) with abundant remnants of ammonites (Andrusov et al. 1955). They are very often associated with microstromatolites.

Manganese mineralization filling the fissures and cavities represents later supergene mobilization and oxidation by meteoric waters (Mikušovce). Manganese ores in these places show higher Mn/Fe ratio than the Fe-Mn crusts (Mišík & Rojkovič 2002). The secondary high-grade ore was formed in fissures and cavities by meteoric water transport from the manganese hardgrounds of dissolved Callovian-Oxfordian red limestone during the Barremian–Aptian time.

Conclusions

The manganese hardgrounds of small extent examined in this study, occurring both, in the Pieniny Klippen Belt (mainly at the base of the Czorzstyn Limestone) and in the Central Western Carpathians (Nedzov Nappe), represent sediments of pelagic up to shallow neritic marine facies with abundant remnants of ammonites.

Manganese-iron crusts and nodules in the Jurassic limestones in the studied area of the Western Carpathians correspond to the recent submarine hardgrounds. They are represented by pyrolusite, romanèchite, manganite, todorokite and goethite. Zoned alternation of the studied manganese oxides and hydroxides with iron hydroxides and calcite is dominant and indicates hydrogenetic accumulation.

The increased contents of Ni, Cu, Co (up to 0.5 wt. %), as well as Mn/Fe ratios (1 to 4) and Si/Al ratios, indicate the hydrogenetic to diagenetic origin of the studied ores. Fe/Mn ratios in the studied manganese crusts and nodules (0.3 to 0.8) are closer to the recent open ocean seamount crusts than to the continental margin seamont crusts. The average organic carbon content in the studied samples (0.20 wt. %) is also closer to the deep ocean nodules than to the continental shelf forms.

REE distribution in the studied manganese crusts with distinct positive Ce anomaly corresponds to hydrogenetic to di-

agenetic origin and it does not indicate the presence of a volcanic source for the formation of the studied manganese mineralization.

Association of the studied manganese mineralization with microstromatolites is distinct and we have to take into account the role of microorganisms in manganese deposition.

The younger manganese mineralization, filling fissures and cavities, consist of dominant manganite and pyrolusite. It represents later supergene mobilization and oxidation by meteoric waters. Manganese ores in these places show higher Mn/Fe ratio than the Mn-Fe crusts. This high-grade ore was formed by meteoric water transport from the manganese hardgrounds of dissolved Callovian-Oxfordian red limestone during the Barremian–Aptian time.

Acknowledgments: The study was supported by Grants 160 of VTP GP and 1/7293/20 of VEGA. Critical comments of the reviewers S. Kasten (Universität Brehmen), K.P. Krajewski (ING PAN Warszawa, Poland), and J. Soták (SAV Banská Bystrica, Slovakia) significantly helped to improve the manuscript. We thank Ľ. Puškelová (Geological Institute of the Slovak Academy of Sciences) for the analyses of a part of rocks and minerals and D. Ozdín (Geological Survey of the Slovak Republic).

References

Andrusov D. 1945: Geological investigations of the inner Klippen Belt in the Western Carpathians. Part IV — Statigraphy of Dogger and Malm. Part V — Stratigraphy of the Cretaceous. *Práce Štát. Geol. Úst.* 13, 1–176 (in Slovak).

Andrusov D., Gorek A. & Nemčok A. 1955: Manganese ore deposits of Slovakia II. Manganese ores of the Pieniny Klippen Belt of the middle part of Váh Valley. *Geol. Sbor. SAV* 6, 1–2, 104–114 (in Slovak).

Aubrecht R., Mišík M., Sýkora M. & Šamajová E. 1998: Controversal klippe of the Czorsztyn Unit in the Bolešovská dolina valley, between Nemšová and Pruské in the Váh river valley. *Miner. Slovaca* 30, 6, 431–442 (in Slovak).

Aubrecht R., Schlögl J. & Mišík M. 2000: Reconstruction of the main direction of the Middle Jurassic extension in Oravicum on the basis of neptunian dykes study in the Czorsztyn Unit — preliminary results. *Manuscript*, *Archive GSSR*, Bratislava 1–37 (in Slovak).

Ballarini, L., Massari, F., Nardi, S. & Scudeler Baccelle L. 1994: Amino acids in the pelagic stromatolites of the Rosso Ammonitico Veronese Formation (Middle-Upper Jurassic, Southern Alps, Italy). In: Bertrand-Sarfati J. & Monty C. (Eds.): Phanerozoic Stromatolites II. *Kluwer Academic Publishers* 279–294.

Banerjee R., Roy S., Dasgupta S., Mukhopadhyay S. & Miura H. 1999: Petrogenesis of ferromanganese nodules from east of the Chagos Archipelago, Central Indian Basin, Indian Ocean. *Marine Geology* 157, 145–158.

Bargar J.R., Tebo B.M. & Villinski J.E. 2000: In situ characterization of Mn(II) oxidation by spores of the marine Bacillus sp strain SG-1. *Geochim. Cosmochim. Acta* 64, 2775–2778.

Birkenmajer K. 1977: Jurassic and Cretaceous lithostratigraphic units of the Pieniny Klippen Belt, Carpathians, Poland. *Stud. Geol. Pol.* 45, 1–158.

Birkenmajer K. 1986: Stages of structural evolution of the Pieniny Klippen Belt, Carpathians. *Stud. Geol. Pol.* 88, 7–32.

Birkenmajer K. 1988: Exotic Andrusov Ridge: its role in plate-tectonic evolution of the West Carpathian Foldbelt. *Stud. Geol. Pol.* 91, 7–37.

Bonatti E., Kraemer T. & Rydell H. 1972: Classification and genesis of submarine iron-manganese deposits. In: Horn D.R. (Ed): Ferromanganese deposits on the ocean floor. *Washington D.C.,* 149–166.

Bonnati E., Zerbi M., Kay R. & Rydell H. 1976: Metalliferous deposits from the Appennine ophiolites: Mesozoic equivalent of modern deposits from oceanic spreading centers. *Geol. Soc. Amer. Bull.* 87, 83–94.

Borchert H. 1980: On the genesis of manganese ore deposits. In: Varentsov I.M. & Grassely G. (Eds.): Geology and geochemistry of manganese. *Akadémiai Kiadó,* Budapest, Vol. II, 13–44.

Corbin J.C., Person A., Iatzoura A., Ferré B. & Renard M. 2000: Manganese in Pelagic carbonates: indication of major tectonic events during the geodynamic evolution of a passive continental margin (the Jurassic European Margin of the Tethys-Ligurian Sea). *Palaeogeogr. Palaeoclim. Palaeoecol.* 156, 123–138.

Cronan D.S., Tichy G. & Mindszenty A. 1999: Paleoenvironments of ferromanganese deposits from Jurassic rocks in Austria. In: Stanley et al. (Eds): Mineral deposits: Processes to processing. *Balkena,* Rotterdam, 1221–1224

Čechovič V. 1942: Manganese ore deposits of Slovakia I. *Práce Štát. Geol. Úst.* 6, 1–26 (in Slovak).

DiStefano P. & Mindszenty A. 2000: Fe-Mn-encrusted ''Kamenitza'' and associated features in the Jurassic of Monte Kumeta (Sicily): subaerial and/or submarine dissolution? *Sed. Geol.* 132, 37–68.

Dragastan O. & Mišík M. 2001: Non-marine Lower Cretceous algae and cyanobacteria from Slovakia. *Geol. Carpathica* 52, 4, 229–237.

Drittenbass W. 1979: Sedimentologie und Geochemie von Eisen-Mangan führenden Knollen und Krusten im Jura der Trento-Zone (östliche Südalpen, Norditalien). *Eclogae Geol. Helv.* 72, 313–345.

Dromart G., Gaillard C. & Jansa L.F. 1994: Deep-marine microbial structures in the Upper Jurassic of Western Tethys. In: Bertrand-Sarfati J. & Monty C. (Eds.): Phanerozoic Stromatolites II. *Kluwer Academic Publishers,* 295–318.

Fan D.L., Hein J.R. & Ye J. 1999: Ordovician reef-hosted Jiaodingshan Mn-Co deposit and Dawashan Mn deposit, Sichuan Province, China. *Ore Geol. Rev.* 15, 135–151.

German K. 1972: Verbreitung und Entstehung Mangan-reicher Gesteine im Jura der Nördlichen Kalpalken. *Tschermaks Miner. Petrogr. Mitt.* 17, 123–150.

Glasby G.P. 2000: Manganese: Predominant role of nodules and crusts. In: Schulz H.D. & Zabel M. (Eds.): Marine geochemistry. *Springer*, Heidelberg-New York, 335–372.

Goodell H.G., Meylan M.A. & Grant B. 1971: Ferromanganese deposits of the South Pacific Ocean, Drake Passage and Scotia Sea. In: J.L. Reid (Ed.): Antarctic Oceanology. *Antarct. Res. Ser.* 15, 27–92.

Halbach P., Scherhag C., Hebisch U. & Marchig V. 1981: Geochemical and mineralogical control of different genetic types of deep-sea nodules from the Pacific Ocean. *Miner. Deposita* 16, 59–84.

Hein J.R., Koschinsky, A. Halbach P., Manheim F.T., Bau M., Kang J-K. & Lubick N. 1997: Iron and manganese oxide mineralization in the Pacific. In: Nicholson K., Hein J.R., Bühn B. & Dasgupta S. (Eds): Manganese mineralization: Geochemistry and Mineralogy of Terrestrial and Marine Deposits. *Geol. Soc. Spec. Publ.* 119, 123–138.

Jenkyns H.C. 1970: Fossil Manganese Nodules from the West Sicilian Jurassic. *Eclogae Geol. Helv.* 63, 741–774.

Jenkyns H.C., Geczy B. & Marshall J.G. 1991: Jurassic manganese carborates of central Europe and the Early Toarcian anoxic

event. *J. Geol.* 99, 137–149.

Jimenez Espinosa R., Jimenez Millan J. & Nieto L. 1997: Factors controlling the genesis of Fe-Mn crusts in stratigraphic breaks of the eastern Betic Cordillera (SE Spain) deduced from numerical analysis of geological data. *Sed. Geol.* 114, 97–107.

Jung H.S. & Lee C.B. 1999: Growth of diagenetic ferromanganese nodules in an oxic deep-sea sedimentary environment, northeast equatorial Pacific. *Marine Geology* 157, 127–144.

Kasten S., Glasby G.P., Schulz H.D., Friedrich G. & Andreev S.I. 1998: Rare earth elements in manganese nodules from the South Atlantic Ocean as indicators of oceanic bottom water flow. *Marine Geology* 146, 33–52.

Koschinsky A. & Halbach P. 1995: Sequential leaching of marine ferromanganese precipitates: Genetic implications. *Geochim. Cosmochim. Acta* 59, 5113–5132.

Kuhn T., Bau M., Blum N. & Halbach P. 1998: Origin of negative Ce anomalies in mixed hydrothermal-hydrogenetic Fe-Mn crusts from the Central Indian Ridge. *Earth Planet. Sci. Lett.* 163, 207–220.

Kullmanová A. & Gašpariková V. 1983: Loc.7 - Hrušové. In: 18th European colloquy on micropaleontology. Excursion guide. *GÚDŠ,* Bratislava, 54–57.

Manheim F.T. 1965: Manganese-iron accumulations in the shallow marine environment. Narragensett Marine Lab. *Publ. 3, Univ. of Rhode Island,* 217–276.

Matsumoto R., Minai Y. & Iijima A. 1985: Manganese content, Cerium anomaly, and rate of sedimentation as clues to characterize and classify deep sea sediments. In: Advances in Earth and Planetary Sciences, Formation of Oceanic Margin. *Terra Sci. Pub.,* Tokyo, 913–939.

Mišík M. 1979: Sedimentological and microfacies study in the Jurassic of the Vršatec (castle) klippe — neptunic dykes, Oxfordian bioherm facies. *Záp. Karpaty, Sér. Geol.* 5, 7–56 (in Slovak).

Mišík M. 1994: The Czorsztyn submarine ridge (Jurassic-Lower Cretaceous, Pieniny Klippen Belt): an example of a pelagic swell. *Mitt. Österr. Geol. Gessel.* 86, 133–140.

Mišík M. & Rojkovič I. 2002: Manganese mineralization in Lednica and Mikušovce, Pieniny Klippen Belt, Slovakia. *Miner. Slovaca* 34, 303–320.

Mišík M. & Sýkora M. 1982: Allodapische Barmsteinkalke im Malm des gebirges Čachtické Karpaty. *Geol. Zbor. Geol. Carpath.* 33, 1, 51–78.

Mišík M. & Sýkora M. 1993: Jurassic submarine scarp breccia and neptunian dykes from the Kyjov-Pusté Pole klippen (Czorsztyn Unit). *Miner. Slovaca* 25, 411–427.

Moffett J.W. 1997: The importance of microbial Mn oxidation in the upper ocean: a comparison of the Sargasso Sea and equatorial Pacific. *Deep-Sea Research Part I — Oceanographic Research Papers,* 44, 1277–1291.

Müller P.J., Hartmann M. & Suess E. 1988: The chemical environment of pelagic sediments. In: Halbach P., Friedrich G. & von Stackelberg U. (Eds): The manganese nodule belt of the Pacific Ocean geological environment, nodule formation, and mining aspect. *Enke Verlag*, Stuttgart, 70–99.

Ohta A., Ishii S., Sakakibara M., Mizuno A. & Kawabe I. 1999: Systematic correlation of the Ce anomaly with the Co/(Ni+Cu) ratio and Y fractionation from Ho in distinct types of Pacific deep-sea nodules. *Geochemical J.* 33, 399–417.

Palumbo B., Bellanca A., Neri R. & Roe M.J. 2001: Trace metal partitioning in Fe-Mn nodules from Sicilian soils, Italy. *Chem. Geol.* 173, 257–269.

Peržel M. 1966: New data on the stratigraphy of the Choč Nappe of the Malé Karpaty Mts. *Geol. Práce, Spr.* 38, 87–97 (in Slovak).

Rakús M. 1987: Condensed facies, hardgrounds and neptunic dykes from the Mesozoic formations of the Western Carpathians. *Unpubl. manuscript*, *GÚDŠ,* Bratislava, 1–20.

Roy S. 1980: Genesis of sedimentary manganese formations — Processes and products in recent and older geological ages. In: Varentsov I.M. & Grassely G. (Eds.): Geology and geochemistry of manganese. *Akadémiai Kiadó*, Budapest, Vol. II, 13–44.

Salaj J. 1987: Rhaetian, its position in the Mesozoic and presumed distribution of the individual sedimentation zones of the Western Carpathians. *Miscell. micropaleont.*, 2/1. *Knihovnička ZPN*, 6a, 123–152 (in Slovak).

Salaj J. 1990: New data about geology and paleogeographic-tectonic evolution of the Klippen and Peri-Klippen zones of the middle part of Váh Valley and their problematics. *Knihovnička ZPN* 9a, 93–168 (in Slovak).

Salaj J. 1997: On the importance of Early Cimmerian tectonic activity at the Liassic/Dogger boundary in the Klippen and Peri-Klippen zones of the Western Carpathians. *Zemní Plyn Nafta* 42, 3, 227–245 (in Slovak).

Savelli C., Marani M. & Gamberi F. 1999: Geochemistry of metalliferous, hydrothermal deposits in the Aeolian arc (Tyrrhenian Sea). *J. Volcanol. Geotherm. Res.* 88, 305–323.

Serdyuchenko D.P. 1980: Precambrian biogenic-sedimentary manganese deposits. In: Varentsov I.M. & Grassely G. (Eds.): Geology and geochemistry of manganese. *Akadémiai Kiadó, Budapest* Vol. II, 61–85.

Schweisfurth R. 1971: Manganknollen im Meer. *Nuturwiss.* 58, 344–347.

Toth J.R. 1980: Deposition of submarine crusts rich in manganese and iron. *Geol. Soc. Amer. Bull.* 91, 44–54.

Usui A., Bau M. & Yamazaki T. 1997: Manganese microchimneys buried in the Central Pacific pelagic sediments: evidence of intraplate water circulation? *Marine Geology* 141, 269–285.

Vera J.A. & Martín-Algarra A. 1994: Mesozoic stratigraphic breaks and pelagic stromatolites in the Betic Cordillera, Southern Spain. In: Bertrand-Sarfati J. & Monty C. (Eds.): Phanerozoic Stromatolites II. *Kluwer Acad. Publ.* 319–344.

Yan B.R., Zhang X.G., Liang D.G., Xu D.Y., Liu Y.F. & Xhang W. 1998: Mechanism and modes of microbial minerogenesis of polymetallic nodules on the ocean floor. *Acta Geol. Sin.* 72, 282 (in English).

Zhang F.S., Lin C.Y., Bian L.Z., Chen J.L., Shen H.T. & Han X.Q. 1997: The discovery of chain-like ultra-microfossils in the manganese nodules from the Pacific Ocean. *J. Trace and Microprobe Techniques* 15, 471–476.

Zydorowicz T. & Wierzbowski A. 1986: Jurassic Fe-Mn concretions in the Czorsztyn Succession (Pieniny Klippen Belt). *Przegl. Geol.* 6, 326–327 (in Polish).